Analytical Methods

Accepted Manuscript

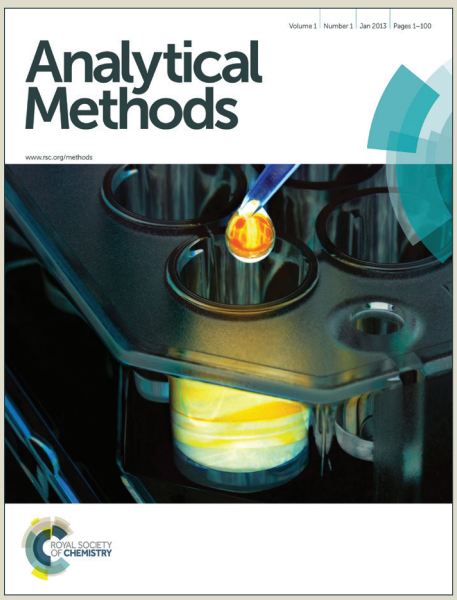

ROYAL SOCIETY OF CHEMISTRY

www.rsc.org/methods

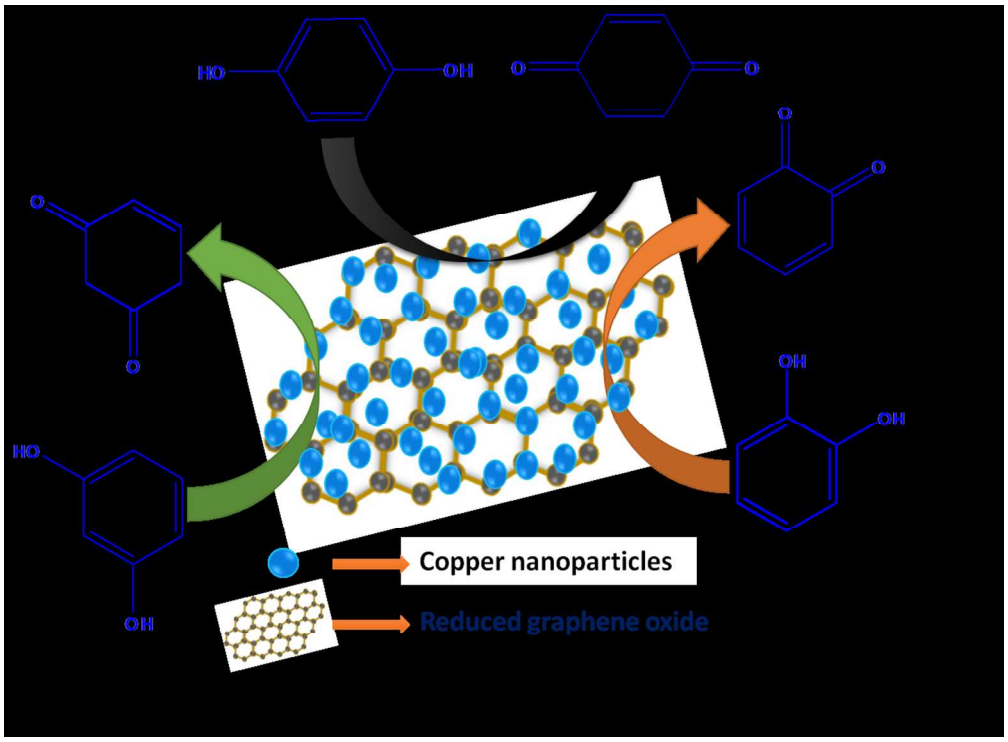

222x162mm (150 x 150 DPI)

Journal Name

RSCPublishing

ARTICLE

Simultaneous and selective electrochemical determination of dihydroxybenzene isomers at reduced graphene oxide and copper nanoparticles composite modified glassy carbon electrode

Cite this: DOI: 10.1039/xoxxoooooox

Received ooth January 2012,
Accepted ooth January 2012

DOI: 10.1039/xoxxoooooox

www.rsc.org/

Selvakumar Palanisamy, [a] Chelladurai Karuppiah, [a] Shen-Ming Chen,*[a] Cheng-Yu Yang, [a] and Prakash Periakaruppan [b]

Herein, we have demonstrated the simultaneous and selective electrochemical determination of dihydroxybenzene isomers at reduced graphene oxide (RGO) and copper nanoparticles (Cu-NPs) composite modified electrode. The RGO/Cu-NPs composite was prepared by a single-step electrochemical reduction method. The synthesized RGO/Cu-NPs composite was characterized by using scanning electron microscope and elemental analysis. Linear sweep voltammetry was employed for the simultaneous determination of hydroquinone (HQ), catechol (CC) and resorcinol (RC). A well defined and more enhanced oxidation peak response is observed for HQ, CC and RC at RGO/Cu-NPs composite than other modified electrodes, which indicates a fast electron transfer of dihydroxybenzene isomers at RGO/Cu-NPs composite. The composite modified electrode shows a high electrocatalytic activity towards the oxidation of HQ, CC and RC. The electrochemical sensor shows a wide linear response in the concentration range of 3 μM to 350 μM, 3 to 350 μM and 12 μM to 200 μM for HQ, CC and RC respectively with a detection limit of 0.012 μM, 0.025 μM and 0.088 μM (S/N=3). In addition, the proposed sensor shows a good selectivity and stability along with good precision and consistency. These obtained results clearly demonstrate that RGO/Cu-NPs composite can be an advanced electrode material for the real time sensing of dihydroxybenzene isomers.

1. Introduction

The simultaneous determination of dihydroxybenzene isomers, hydroquinone (HQ), catechol (CC) and resorcinol (RC), have received tremendous interest due to their key role in antioxidant, pesticide, cosmetics, dyes, medicine, flavoring agents, tanning, photography chemicals and pharmaceutical industries.[1, 2] Moreover, they have also been certified as a toxic environmental pollutant by the U.S Environmental Protection (EPA) Agency and the European Union (EU) due to their low degradability and highly toxic impact on biological systems including humans and animals.[3] Till now, many analytical methods have been used for simultaneous determination of these dihydroxybenzene isomers, including high

performance liquid chromatography, spectrometry, fluorescence, chemiluminescence and electrochemical methods.[4-9] Among the various analytical methods, electrochemical methods have paid more attention to the simultaneous determination of dihydroxybenzene isomers owing to its inexpensive, fast response, user friendly with high sensitivity and selectivity.[10] However, the individual or simultaneous determination of dihydroxybenzene isomers at the conventional electrodes are very difficult and challenging task due to their similar structural characteristic properties and overlapping of signals of each isomer leads to fouling of the signals on electrodes.[11, 12] To overcome these problems, modified electrodes have been used for the individual or simultaneous determination of HQ, CC and RC. To date, various nanomaterials including carbon nanomaterials, conducting and redox active polymers and so on have been employed in the modified electrodes to attain the better sensitivity and selectivity for individual or simultaneous determination of dihydroxybenzene isomers.[13-19]

Reduced graphene oxide (RGO) has got great interest in the field of electrochemical sensors owing to its higher surface area, high chemical stability and unique electronic and mechanical properties than other carbon nanomaterials like carbon nanotubes, graphene oxide (GO), fullerenes, carbon black etc.,[19-21] Currently, a plenty of nanostructured materials have been used with RGO to enhance the sensing properties of RGO in various potential disciplines including electrochemical sensors, energy storage and biomedical applications.[22] Among various nanostructured materials, particularly, copper nanoparticles (Cu-NPs) have received a significant interest, due to their excellent electrocatalytic ability that has been widely employed for the various potential disciplines including electrochemical sensors and biosensors.[22, 23] Whereas chemical methods have been largely employed for the fabrication of RGO/Cu-NPs composite,[24, 25] electrochemical fabrications of RGO/Cu-NPs composites are seldom reported. The electrochemical fabrication of RGO/Cu-NPs is considered as a simple and cost-effective method compared to chemical methods, which involve hydrazine and sodium borohydride.[26] In our previous studies, we have demonstrated that RGO/metal nanoparticle or metal oxide composites can be prepared by the simple electrochemical reduction of GO and the corresponding metal salt solutions in room temperature without the addition of any external reducing agents.[27-29] Herein, we have fabricated RGO/Cu-NPs composite by using the same strategy, typically a single-step electrochemical reduction of GO and Cu (II) ions. In addition, to the best of our knowledge, this is the first report for the simultaneous electrochemical determination of dihydroxybenzene isomers by using RGO/Cu-NPs composite modified electrode.

In this paper, we have fabricated RGO/Cu-NPs composite by simple reduction of GO and Cu (II) ions by using electrochemical method. The fabricated RGO/Cu-NPs composite modified electrode was used for the simultaneous determination of dihydroxybenzene isomers like HQ, CC and RC. The proposed electrode shows a more enhanced response towards simultaneous determination of HQ, CC and RC than that of RGO and Cu-NPs modified electrodes. In addition, we have also demonstrated the practicality of the modified electrode for the individual and simultaneous determination of HQ, CC and RC in tap water samples.

2. Experimental

Materials and methods

Graphite powder was purchased from Sigma Aldrich. Copper nitrate trihydrate, 99.8% [$Cu(NO_3)_2.3H_2O$], potassium nitrate, 99.8% (KNO_3), catechol, 99% , hydroquinone, 99% and resorcinol, 99% were purchased from Wako Pure Chemical Industries, Ltd and used

as received. The phosphate buffer solution of pH 7 (PBS) was prepared by using 0.1 M Na_2HPO_4 and NaH_2PO_4 solutions and other pH solutions were prepared using PBS with 0.5 M H_2SO_4 and 2 M NaOH. All other chemicals used were of analytical grade and all solutions were prepared using Millipore water.

All electrochemical measurements were carried out in a three-electrode system with a CHI 750a electrochemical analyzer (CH instruments). Linear Sweep Voltammetry (LSV) was performed by CHI 750a electrochemical analyzer (CH instruments). Surface morphological studies were carried out using Hitachi S-3000 H scanning electron microscope. An energy-dispersive X-ray (EDX) spectrum was recorded using HORIBA EMAX X-ACT attached with Hitachi S-3000 H scanning electron microscope. Powder X-ray diffraction (XRD) studies were performed in a XPERT-PRO (PANalytical B.V., The Netherlands) diffractometer using Cu Kα radiation. Electrochemical impedance spectroscopy (EIS) studies were performed by using IM6ex ZAHNER (Kroanch, Germany). The modified Glassy carbon electrode (GCE) was used as a working electrode. Ag/AgCl electrode (Sat. KCl) and platinum wire were used as reference and counter electrodes, respectively. All measurements were carried out at room temperature and the electrolyte solutions were kept under N_2 atmosphere for 5-10 min prior to all electrochemical measurements.

Fabrication of RGO/Cu-NPs composite modified electrode

Graphite oxide was synthesized from raw graphite powder using modified Hummer's method [30] and it was converted into GO upon subjecting its aqueous solution to ultrasonication for 30 min. RGO/Cu-NPs composite was synthesized by simple electrochemical method. About 8 µL of GO solution (optimized concentration) was drop cast onto a GCE surface and allowed to dry in an air oven. The GO modified GCE was immersed into an electrochemical cell containing 0.5 mM $Cu(NO_3)_2.3H_2O$ and 1 mM KNO_3 solution. Consequently, RGO/Cu-NPs composite obtained by the 20 successive cycles of CVs were performed in the potential range between 0.8 to -1.4 V at the scan rate of 100 mVs^{-1}. The RGO/Cu-NPs modified GCE was gently rinsed with distilled water to remove the loosely bound Cu-NPs particles. The fabricated RGO/Cu-NPs composite modified GCE was used for further experiments and stored at room temperature under dry condition. The schematic representation for the fabrication of RGO/Cu-NPs composite is shown in Fig. 1.

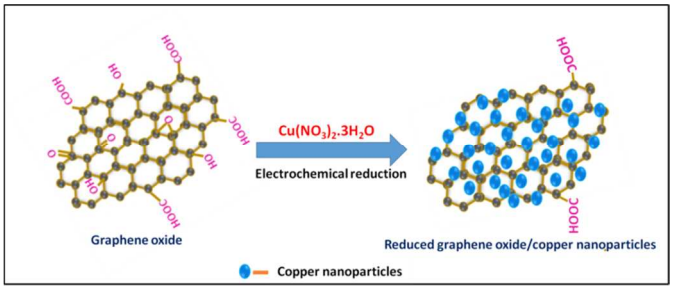

Fig. 1 A schematic representation of single step electrochemical fabrication of RGO/Cu-NPs composite.

3. Results and Discussion

Formation mechanism of RGO-Cu-NPs composite

Fig. 2 shows the electrochemical reduction of GO modified electrode in the electrochemical cell containing 0.5 mM $Cu(NO_3)_2.3H_2O$ and 1 mM KNO_3 solution. During the first cathodic potential scan, a large cathodic peak appears with an onset potential of −0.70 V, which is attributed to the reduction of oxygen containing groups at the GO basal plane.[26, 29] Besides, during the first cathodic potential scan, a good cathodic peak is observed with an onset potential of 0.03 V, indicating the formation of metallic Cu^0 from Cu^{2+} ions.[31, 32] Upon reverse sweeping toward positive direction, a sharp anodic peak is observed at 0.3 V, due to the oxidation of metallic Cu^0 to Cu^{2+} ions.[32, 33] The oxidation potential of Cu nucleation starts at the same potential with respect to its equilibrium potential of where Cu-

NPs already deposited (0.3 V) and the results are very similar to the electrodepostion of Cu-NPs as reported previously.[33] However, no anodic peak (0.3 V) of Cu is observed when GO is electrochemically reduced in the same potential window at KNO_3 solution (Fig. 2 inset). This provides further evidence for the formation of Cu^{2+} in the solution during the electrochemical fabrication of Cu-NPs on RGO surface.

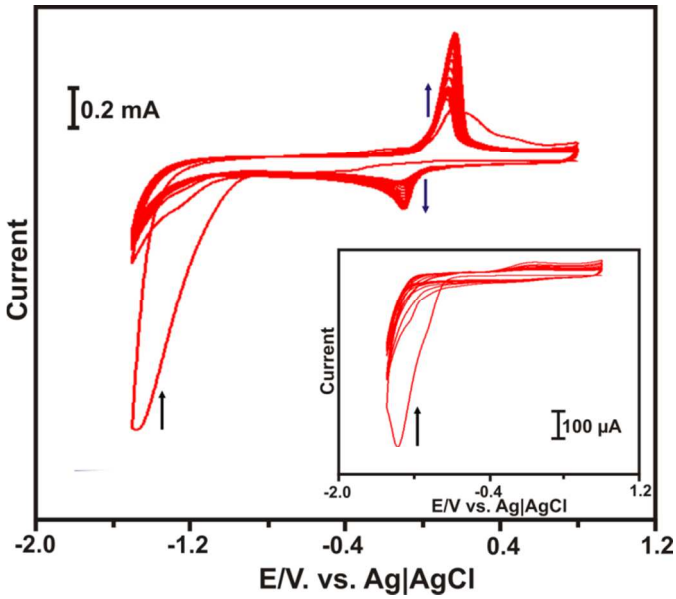

Fig. 2 20 consecutive cyclic voltammograms performed at GO modified GCE in 0.5 mM $Cu(NO_3)_2.3H_2O$ + 1 mM KNO_3 solution at the scan rate of 50 mV s^{-1}. Inset shows the 20 consecutive cyclic voltamograms of GO modified electrode in 1 mM KNO_3 solution at the scan rate of 50 mV s^{-1}.

The possible mechanism for the formation of Cu-NPs on the RGO surface can be expressed by the following equation as reported previously. [31, 33]

$$Cu^{2+} + NO_3^- \rightarrow Cu^{0+} NO_3^- + 2\,e^- \quad (1)$$

Characterizations

Fig. 3 shows the SEM image of RGO (A), Cu-NPs (B), RGO/Cu-NPs composite (C) and the EDX profile for the RGO/Cu-NPs (D). As shown in Fig. 3C, Cu-NPs are distributed uniformly on the RGO sheets with an average diameter of about 80 nm. The morphology of Cu-NPs on RGO surface is in good agreement with Cu-NPs electrodeposited on the bare surface (Fig. 3B). RGO depicts its exfoliated and typical wrinkled surface morphology with closely connected ultrathin sheets (Fig. 3A). It is notable that Cu-NPs are closely attached on the RGO sheets without any dislocation (Fig. 3C inset), which confirms that the electrochemical reduction method does not affect the morphology of Cu-NPs on RGO. The fabricated RGO/Cu-NPs composite is further confirmed by EDX. It can be seen from Fig. 3D that a strong peak of Cu appears at 0.9 eV which confirms the formation of Cu-NPs on RGO surface. These findings confirm the formation of RGO/Cu-NPs composite.

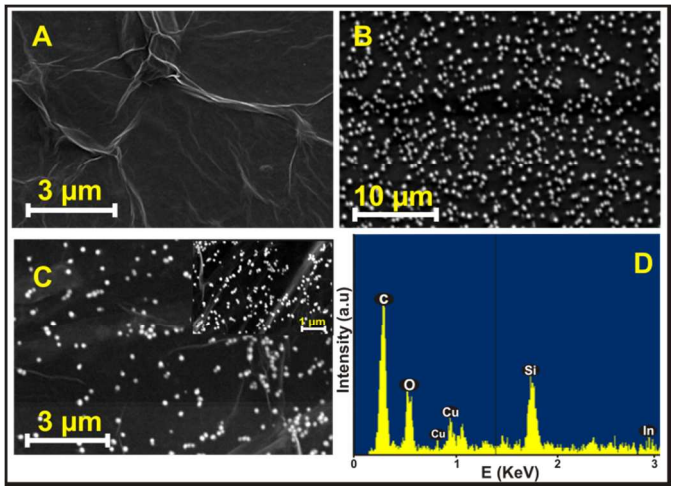

Fig. 3 A Typical SEM image of RGO (A), Cu-NPs (B), RGO/Cu-NPs composite (C) and EDX profile for RGO/Cu-NPs composite (D). Inset in 1C shows the higher magnification of RGO/Cu-NPs composite.

Electrochemical impedance spectroscopy (EIS) is an efficient method to probe the impedance changes of the electrode surface during the medication process. Fig. 4A shows the EIS of GO (a), Cu-NPs (b), RGO (c) and RGO/Cu-NPs modified GCEs (d) in PBS containing 5 mM $Fe(CN)_6^{3-}/Fe(CN)_6^{4-}$. The impedance changes of the electrode surface can be calculated by an equivalent circuit of Randles model (Fig. 4A inset). This equivalent circuit

shows the electron-transfer resistance (R_{ct}), the Warburg impedance (Z_w), the electron transfer resistance of the electrolyte (R_s), and interfacial capacitance (C_{dl}). Generally, a semicircle part of the Nyquist plot results from the parallel combination of R_{et} and C_{dl} resulting from electrode impedance.

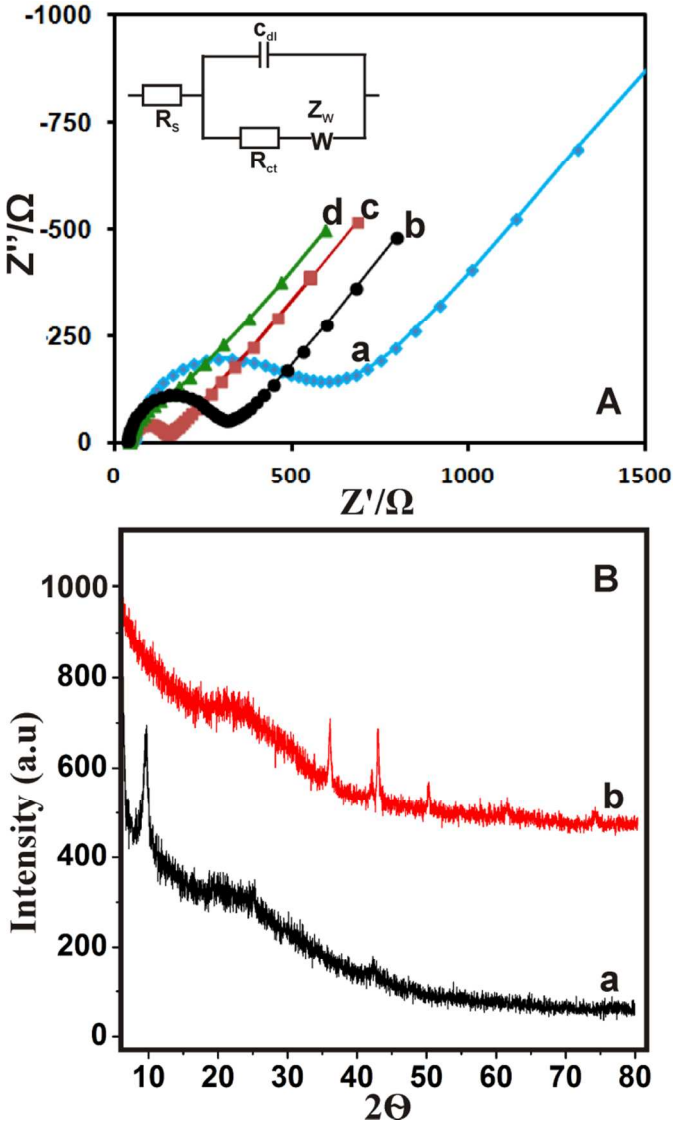

Fig. 4 A) EIS of GO (a), Cu-NPs (b), RGO (c) and RGO/Cu-NPs modified GCEs in PBS containing 5 mM $Fe(CN)_6^{3-}/Fe(CN)_6^{4-}$. Inset shows the equivalent circuit of Randles model. B) Typical XRD patterns of GO (a) and RGO–Cu-NPs composite (b).

The semicircle diameter represents the electron-transfer resistance, which dominates the electron transfer kinetics of the redox probe at the electrode interface. Meanwhile, the linear part at lower frequencies corresponds to the diffusion process. The GO modified GCE exhibits a large semicircle due to the low conductivity that leads to the poor electron transfer between solution and electrode interface. That the diameter of the semicircle greatly decreases in the EIS of RGO is attributed to the excellent conductivity of RGO and it can improve electron transfer kinetics between solution and electrode surface. The value of R_{et} further decreases after the introduction of Cu-NPs on RGO, indicating that RGO/Cu-NPs can improve the electron transfer kinetics to a large extent compared to RGO and Cu-NPs.

The formation of RGO/Cu-NPs composite was further confirmed by XRD analysis. Fig. 4B shows the XRD patterns of GO (a) and RGO–Cu-NPs composite (b). The exfoliated GO exhibits a sharp diffraction peak at 9.9º, which is attributed to the prevailing of stacking order as in graphite.[34] On the other hand, in RGO/Cu-NPs composite, three distinct diffraction XRD peaks are observed at 44.3º, 50.7º and 74.1º, which are attributed to the (1 1 1), (2 0 0) and (2 2 0) planes of the face centered cubic Cu-NPs.[35] The typical peaks of RGO-Cu-NP composite at 2□ of 26º and 43º correspond to the characteristic peaks of (002) and (100) plane reflections of graphite from the reduced graphene oxide.[35] The XRD peak at 36.5º is attributed to the impurity peak of Cu_2O. The reason may be due to the little oxidation of Cu-NPs. These results confirm the formation of RGO/Cu-NPs composite.

Electrocatalytic activity of the mixed components of HQ, CC and RC

Cyclic voltammetry was used to evaluate the electrochemical behavior of different modified electrodes. Fig. 5A shows the cyclic voltammetry response of bare (a), Cu-NPs (b), RGO (c) and

RGO/Cu-NPs (d) modified electrodes in the absence of 200 µM HQ, CC and RC in PBS at the scan rate of 50 mV s^{-1}.

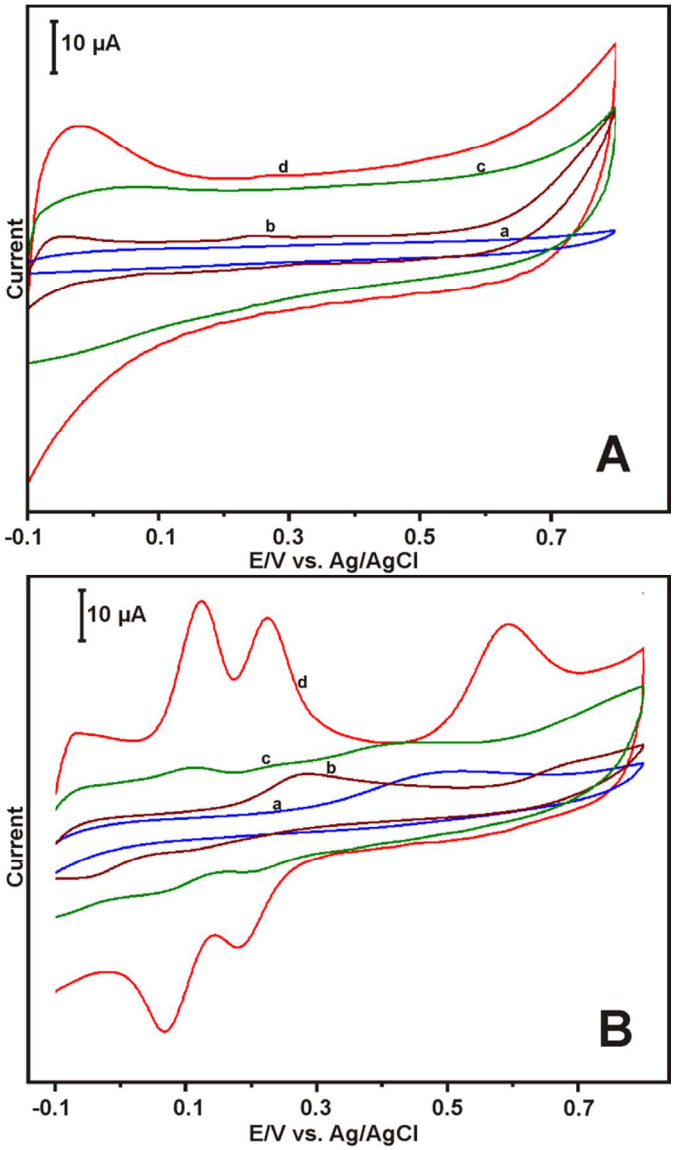

Fig. 5 A) Cyclic voltammograms of bare (a), Cu-NPs (b), RGO (c) and RGO/Cu-NPs (d) modified electrodes in the absence of HQ, CC and RC in PBS at the scan rate of 50 mV s^{-1}. B) At the same conditions, bare (a), Cu-NPs (b), RGO (c) and RGO/Cu-NPs (d) modified electrodes in the presence of a mixture of 100 µM HQ, CC and RC.

As shown in Fig. 5A, in the absence of dihydroxybenzene isomers, no noteworthy peak response is observed at bare (a) and RGO (c) modified electrodes, indicating that these electrodes are electrochemically inactive in this potential window. Whereas, Cu-NPs (b) modified electrode exhibits a sharp anodic peak at -0.044 V and also a small anodic peak is observed at 0.25 V in the absence of isomers owing to the presence of Cu-NPs. The anodic peaks of Cu-NPs show a positive shift (0.268 V, -0.022 V) at RGO/Cu-NPs (d) composite. The results clearly indicate that the anodic peaks of Cu-NPs and RGO/Cu-NPs do not appear where the peaks of HQ and CC appeared.

Fig. 5B depicts the cyclic voltammetric response of bare (a), Cu-NPs (b), RGO (c) and RGO/Cu-NPs (d) modified electrodes in the presence of 200 µM HQ, CC and RC in PBS at the scan rate of 50 mV s^{-1}. A broad oxidation peak appears at 0.470 V at bare electrode, which is attributed to the oxidation of CC and HQ and no oxidation peak appears for RC. The result clearly indicates that the bare GCE is not suitable for the simultaneous determination of HQ, CC and RC. At the Cu-NPs modified electrode, two oxidation peaks appear at 0.294 V and 0.720 V respectively, which indicate the overlapping peaks of HQ and CC (0. 294 V) and oxidation peak of RC (0.720 V). In the same potential window at the RGO modified electrode, a weak redox peaks appear for HQ at 0.115/0.072 V and CC at 0.236/ 0.205 V; an irreversible peak for RC at 0.426 V. However, well separated peaks are observed for HQ, CC and RC at RGO/Cu-NPs composite modified electrode. It can be seen that two redox peaks appear for HQ and CC and one irreversible oxidation peak appear for RC at RGO/Cu-NPs electrode in the presence of dihydroxybenzene isomers. Three well defined and clearly separated oxidation peaks are observed at 0.125 V, 0.225 V and 0.594 V for HQ, CC and RC, respectively. Moreover, a sharp anodic peak is observed at -0.022 V due to the presence of Cu-NPs on RGO.

The peak separations (ΔE_p) for HQ and CC and CC and RC are about 0.10 V and 0.369 V, respectively. It is clear that the anodic peaks of HQ, CC and RC can be effectively differentiated at

RGO/Cu-NPs modified electrode compared with RGO and Cu-NPs modified electrode. In addition, the peak current intensities of HQ, CC and RC also increase about 12 folds at the RGO/Cu-NPs modified electrode compared to RGO modified electrodes. The reason is due to the presence of Cu-NPs on RGO, which effectively increases the active sites that enhance the electrocatalytic activity and hence better peak separation of HQ, CC and RC. Moreover, the presence of RGO may significantly increase the effective electrode surface area thus greatly transfer the electron transfer between species and the electrode surface under the diffusion conditions. The results clearly indicate that the RGO/Cu-NPs modified electrode possesses a high catalytic activity with the better peak separation of HQ, CC and RC compared to RGO and Cu-NPs modified electrodes.

Effect of Scan rate and pH

The effect of scan rate on the cyclic voltammetric response of 200 µM HQ, CC and RC mixture in PBS was examined at different scan rates. Fig. 6A shows cyclic voltammograms obtained for the oxidation of 200 µM HQ, CC and RC at RGO/Cu-NPs modified electrode at the scan rates from 10 to 150 mV s^{-1}. The oxidation peak current (I_{pa}) of HQ, CC and RC increase linearly with the square roots of scan rates from 10–150 mVs^{-1} (Fig. 6A inset), indicating the electrochemical oxidation of HQ, CC and RC on RGO/Cu-NPs composite modified electrode, which is a typical diffusion–controlled electrochemical process.[36]

Fig. 6B depicts the effect of pH at RGO/Cu-NPs modified electrode in the different pH solution containing 200 µM of HQ, CC and RC. It can be seen that the oxidation peak potential of HQ, CC and RC shifts negatively with increasing pH from 3 to 9, indicating that the protons are involved in the oxidation of HQ, CC and RC (Fig. 6B inset).

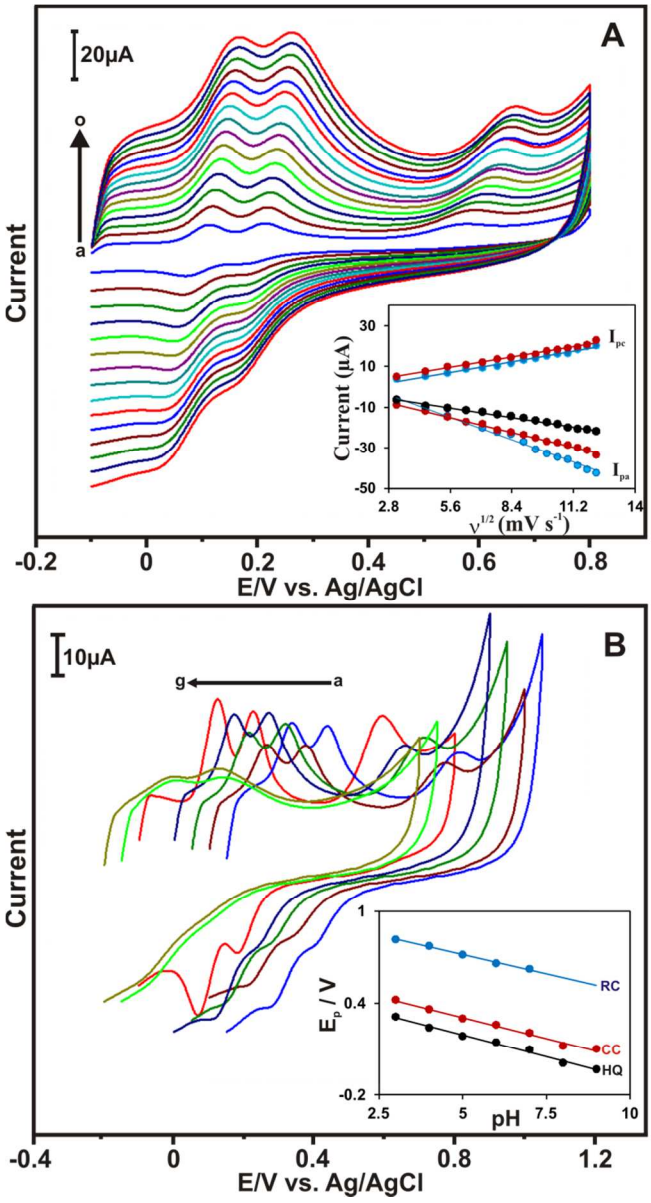

Fig. 6 A) The cyclic voltammograms obtained at RGO/Cu-NPs composite modified electrode in PBS containing 200 µM HQ, CC and RC at different scan rates (10 to 150 mV s^{-1}). The corresponding linear plot for the square root of scan rates vs. peak current response of HQ, CC and RC (inset). B) The cyclic voltammograms of RGO/Cu-NPs composite modified electrode for a mixture of 200 µM HQ, CC and RC in different pH solutions at the scan rate of 50 mV s^{-1}. Inset shows the linear dependence of pH vs. peak potential of HQ, CC and RC.

The linear regression equations are calculated for HQ, CC and RC; oxidation peak potential (E_{pa}) = - 0.0566 pH + 0.4738 (R^2 = 0.9916), E_{pa} = - 0.0551 pH + 0.5814 (R^2 = 0.9901) and E_{pa} = - 0.050 pH + 0.9678 (R^2 = 0.9947), respectively. These obtained slope values of HQ, CC and RC are nearly close to the theoretical value of −58.6 mV/pH, indicating that an equal number of protons and transferred electrons are involved in the oxidation of HQ, CC and RC at RGO/Cu-NPs modified electrode.[36] The maximum I_{pa} appears at pH 7 and then decreases with further increase and decrease of pH. Hence, pH 7 is selected as an optimum for the simultaneous oxidation of HQ, CC and RC.

Simultaneous and selective determination of HQ, CC and RC

The LSV was used to evaluate the simultaneous and selective electrochemical detection of dihydroxybenzene isomers at RGO/Cu-NPs modified electrode, due to its higher sensitivity and selectivity than that of cyclic voltammetry. The selective determination of HQ, CC and RC in their mixed components was performed by changing the concentration of one component and keeping the concentrations of the other two isomers constant. Fig. 7A shows the LSV of different concentrations of the HQ on PBS with a constant 50 µM CC and 75 µM RC. The I_{pa} increases with increasing the concentration of HQ from 5 to 250 µM, where as the I_{pa} of CC and RC are almost constant. The obtained result clearly indicates that the RGO/Cu-NPs modified electrode can easily differentiate these three components when the concentration of HQ is sixteen times higher than that of CC and RC.

As can be seen in Fig. 7B, LSV recorded for different concentrations of CC in the presence of 50 µM HQ and 75 µM RC. The I_{pa} of CC linearly increases with increasing concentrations of CC while I_{pa} of HQ and RC are almost constant. Similarly, the concentration of RC was changed in the presence of 50 µM HQ and CC. As shown in Fig. 7C, the I_{pa} of RC linearly increases upon increasing the RC concentrations. The response current of HQ and CC are constant even in the presence of higher concentration of RC in the solution. Hence, the results suggest that the RGO/Cu-NPs composite modified electrode is more suitable electrode system for the simultaneous determination of HQ, CC and RC. LSV was also recorded for the simultaneous determination of a ternary mixture containing different concentrations of HQ, CC and RC at RGO/Cu-NPs composite modified electrode. As shown in Fig. 7D, the I_{pa} increases linearly with increasing the concentration of HQ, CC and RC. The peak to peak separation of these dihydroxybenzene isomers is well separated up to higher concentration levels with a potential difference of 0.10 V and 0.371 V for the E_{pa} of HQ, CC and CC, RC respectively. The linear response for HQ, CC and RC is found in the concentration range of 3 µM to 350 µM, 3 to 350 µM and 12 µM to 200 µM, respectively.

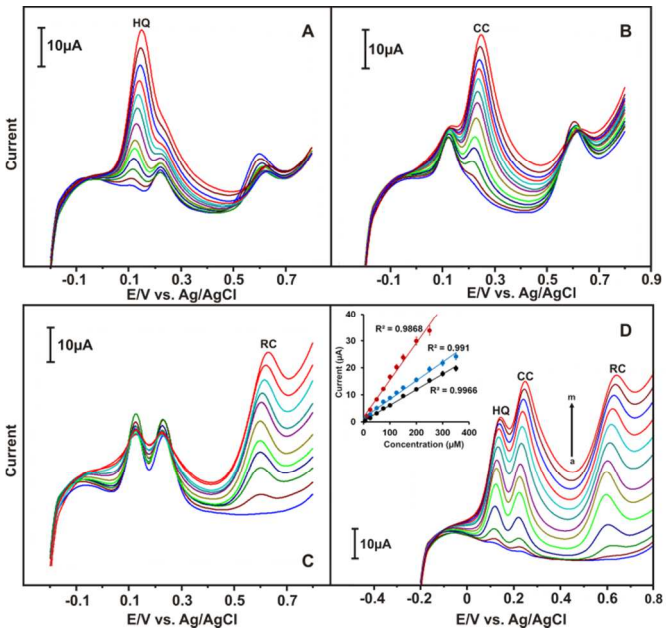

Fig. 7 (A) LSV responses of RGO/Cu-NPs composite modified electrode for 3 to 350 µM of HQ in the presence of 50 µM CC and 75 µM RC in N_2 saturated PBS at 50 mV s^{-1} scan rate. B) At the same conditions, LSV responses of RGO/Cu-NPs composite modified electrode in PBS saturated with N_2 containing 3 to 350 µM CC in the presence of 50 µM HQ and 75 µM RC. C) LSV responses

of RGO/Cu-NPs composite modified electrode for 12 to 200 μM RC in the presence of 50 μM HQ and CC. D) LSVs obtained for the simultaneous electrochemical detection of HQ, CC (3 μM to 350 μM) and RC (12 μM to 200 μM) at RGO/Cu-NPs composite modified electrode (a-m). Inset shows the calibration plot for I_{pa} vs. [HQ], [CC] and [RC]. Error bar shows the relative standard deviation of 3 measurements.

The sensitivity for HQ, CC and RC was calculated from the fitted regression equation as 0.87 ± 0.01 $\mu A \mu M^{-1}$ cm^{-2} , 0.72 ± 0.008 $\mu A \mu M^{-1}$ cm^{-2} and 1.72 ± 0.006 $\mu A \mu M^{-1}$ cm^{-2} respectively. The limit of detection (LOD) was calculated for dihydroxybenzene isomers as 0.032 μM (HQ), 0.025 μM (CC) and 0.088 μM (RC), (S/N=3). The obtained results suggest that the fabricated sensor shows a good linear range response, good sensitivity along with low LOD for the detection of dihydroxybenzene isomers.

Selectivity, storage stability, repeatability and reproducibility of the sensor

The selectivity of the sensor towards the other suspicious species was investigated by LSV. The response of the RGO/Cu-NPs composite modified electrode was examined in PBS containing 75 μM HQ, 75 μM CC, 75 μM RC in the presence of potentially interfering species like 10 mM Cu^{2+}, Ca2+, Zn^{2+}, K^{+}, Na^{+}, SO_4^{2-} and Cl^{-}. Obviously, the interfering species do not affect the response of HQ, CC and RC signals at the RGO/Cu-NPs composite modified electrode, authenticating the good selectivity and good anti-interference ability of the proposed sensor.

The storage stability of the fabricated sensor was examined by LSV with the response current of the sensor to PBS containing 75 μM HQ, 75 μM CC and 75 μM RC and was monitored periodically. The modified electrode retains the original response current of about 93.2 %, 94.5% and 90.3% for HQ, CC and RC respectively, after 25 days. Under the optimized conditions, the relative standard deviation (RSD %) of the RGO/Cu-NPs composite modified electrode in 10 successive measurements for HQ, CC and RC are 1.2 %, 2.3 % and 2.8 %, respectively. The 4 set of RGO/Cu-NPs composite modified electrode was prepared independently under the same conditions, which show an acceptable reproducibility for HQ, CC and RC with the RSD of 3.2%, 1.7 % and 2.8 %, respectively. The result clearly reveals that the modified electrode possesses a high storage stability along with good repeatability and reproducibility, which is attributed to the high stability of the RGO/Cu-NPs composite.

Real sample analysis

The fabricated RGO/Cu-NPs composite electrode was examined for the simultaneous determination of HQ, CC and RC in the tap water samples using the standard addition method. The LSV was used to evaluate the practicality of the sensor. The experimental conditions are same as that discussed in Fig. 7. The obtained recovery results are shown in Table 1. A good recovery (97.0% to 104.4%) of dihydroxybenzene isomers clearly authenticates that the developed sensor can be used as a potential candidate for the individual and simultaneous determination of HQ, CC and RC in environmental samples.

Conclusions

In conclusion, this work demonstrates that RGO/Cu-NPs composite modified electrode can effectively be employed for the simultaneous electrochemical determination of dihydroxybenzene isomers and the RGO/Cu-NPs composite can be prepared by a single-step electrochemical reduction method. The surface morphological studies reveal that Cu-NPs with an average diameter of 80 nm are uniformly deposited on the RGO surface, indicating that electrochemical reduction is a simple method for the fabrication of RGO/Cu-NPs composite. An enhanced peak current response of

dihydroxybenzene isomers is observed at RGO/Cu-NPs composite modified electrode compared to RGO and Cu-NPs modified electrodes. The fabricated composite electrode shows a good sensitivity, selectivity along with a wider linear range of detection of HQ, CC and RC. The good practicality of the sensor clearly reveals that it can be used as a potential candidate for the quantitative determination of dihydroxybenzene isomers.

Acknowledgments

This project was supported by the National Science Council and the Ministry of Education of Taiwan (Republic of China).

Notes and references

[a] Electroanalysis and Bioelectrochemistry Lab, Department of Chemical Engineering and Biotechnology, National Taipei University of Technology, No. 1, Section 3, Chung-Hsiao East Road, Taipei 106, Taiwan, ROC. E-mail: smchen78@ms15.hinet.net;

Fax: +886-2-27025238; Tel: +886-2-27017147.

[b] Post Graduate and Research Department of Chemistry, Thiagarajar College, Madurai-625009, Tamilnadu, India.
E-mail: kmpprakash@gmail.com

1 T. Xie, Q. Liu, Y. Shi and Q. Liu, *J. Chromatogr. A*, 2006, **1109**, 317-321.

2 H.S. Yin, Q.M. Zhang, Y.L. Zhou and Q. Ma, *Electrochim. Acta*, 2011, **56**, 2748-2753.

3 M. Blaut, A. Braune, S. Wunderlich, P. Sauer, H. Schneider and H. Glatt, *Food Chem. Toxicol*., 2006, **44**, 1940-1947.

4 L.J. Zhao, B.Q. Lu, H.Y. Yuan, Z.D. Zhou and D. Xiao, *Sensors,* 2007, **7**, 578 588.

5 G. Marrubini, E. Calleri, T. Coccini, A.F. Castoldi and L. Manzo, *Chromatographic*, 2005, **62**, 25-31.

6 Afkhami and H.A. Khatami, *J. Anal. Chem*., 2001, **56**, 429-432.

7 Nasr, G. Abdellatif, P. Canizares, C. Saez, J. Lobato and M.A. Rodrigo, *Environ. Sci. Technol.*, 2005, **39**, 7234-7239.

8 P. Yang, Q.Y. Zhu, Y.H. Chen and F.W. Wang, *J. Appl. Polym. Sci*., 2009, **113**, 2881-2886.

9 S.J. Li, Y. Xing and G.F. Wang, *Microchim. Acta*, 2012, **176**, 163-168.

10 Z. Hong, L. Zhou, J. Li and J. Tang, *Electrochim. Acta* , 2013, **109**, 671-677.

11 W. Sun, Y. Wang, Y. Lu, A. Hu, F. Shi and Z. Sun, *Sens. Actuators B* , 2013, **188**, 564-570.

12 Zhang, L. Zeng, X. Zhu, C. Yu, X. Zuo, X. Xiao and J. Nan, *Anal. Methods*, 2013, **5**, 2203-2208.

13 Bu, X. Liu, Y. Zhang, L. Li, X. Zhou and X. Lu, *Colloids Surf. B*, 2011, **88**, 292-296.

14 X. Yuan, D. Yuan, F. Zeng, W. Zou, F. Tzorbatzoglou, P. Tsiakaras and Y. Wang, *Appl. Catal. B*, 2013, **129**, 367-374.

15 Z.S. Yang, G.Z. Hu, Y.C. Liu, J. Zhao and G.C. Zhao, *Can J. Anal Sci. Spect*., 2006, **52**, 11.

16 L.Y. Chen, Y.H. Tang, K. Wang and C.B. Liu, *Electrochem. Commun.,* 2011, **13**, 133-1337.

17 X. Feng, Y. Shi and Z. Hu, *Mater. Chem. Phy*., 2011, **131**, 72-76.

18 J. Wang and N.F. Hu, *Bioelectroch. Bioener*., 1999, **48**, 117-127.

19 A.K. Geim and K.S. Novoselov, *Nat. Mater*., 2007, **6**, 183-191.

20 M.J. Allen, V.C. Tung and R.B. Kaner, *Chem. Rev.*, 2010, **110**, 132-145.

21 Y. Shao, J. Wang, H. Wu, J. Liu, I.A. Aksay and Y. Lin, *Electroanalysis*, 2010, **22**, 1027-1036.

22 X. Huang, Z. Yin, S. Wu, X. Qi, Q. He, Q. Zhang, Q. Yan, F. Boey and H. Zhang, *small*, 2011, **7**, 1876-1902.

23 X. Huang, X. Qi, F. Boeya and H. Zhang, *Chem. Soc. Rev*., 2012, **41**, 666-686.

24 T. Wu, J. Gao, X. Xu, W. Wang, C. Gao and H. Qiu, *Nanotechnology*, 2013, **24**, 215604-215614.

25 Q. Chen, L. Zhang and G. Chen, *Anal. Chem*., 2012, **84**, 171-178.

26 H.L. Guo, X.F. Wang, Q.Y. Qian, F.B. Wang and X.H. Xia, *ACS Nano*, 2009, **3**, 2653-2659.

27 S. Palanisamy, S. Ku and S.M. Chen, *Microchim. Acta,* 2013, **180**, 1037-1042.

28 S. Palanisamy, C. Karuppiah and S.M. Chen, *Colloids Surf. B*, 2014, **114**, 164-169.

29 S. Palanisamy, S.M. Chen and R. Sarawathi, *Sens. Actuators B*, 2012, **372**, 166-167.

30 W.S. Hummers and R.E. Offeman, *J. Am. Chem. Soc*., 1958, **80**, 1339.

31 Grujicic and B. Pesic, *Electrochim. Acta*, 2002, **47**, 2901-2912.

32 L. Huang, E.S. Lee and K.B. Kim, *Colloids Surf. A: Physicochem. Eng. Asp*., 2005, **262**, 125-131.

33 O. Ghodbane, L. Roue and D. Belanger, *Electrochim. Acta*, 2007, **52**, 5843-5855.

34 Z. Wang, X. Zhou, J. Zhang, F. Boey, and H. Zhang, *J. Phys. Chem. C,* 2009, **113**, 14071–14075.

35 Y. Zhang, H. Tang, X, Ji, C, Li, L. Chen, D. Zhang, X. Yang, and H. Zhang, *RSC Adv*., 2013, **3**, 26086-26093

36 X. Cao, X. Cai, Q. Feng, S. Jia and N. Wang, *Anal. Chim. Acta*, 2012, **752**, 101-105.

Table. 1 Determination of individual and mixtures of HQ, CC and RC in tap water samples at RGO/Cu-NPs composite modified electrode (n=3).

Sample labeled	Added			Found[a]			Recovery (%)		
	HQ	CC	RC	HQ	CC	RC	HQ	CC	RC
A	25	-	-	24.8	-	-	99.2	-	-
B	-	50	-	-	49.1	-	-	98.2	-
C	-	-	50	-	-	48.6	-	-	97.2
1	25	50	-	48.8	49.8	-	97.6	99.6	-
2	25	50	50	72.8	100.4	49.0	97.1	100.4	98.0

[a] Standard addition method.

A, B and C are the spiked diluted samples of individual compounds (HQ, CC and RC) in tap water.

1 and 2 are the spiked diluted samples of mixtures of HQ, CC and RC in tap water.

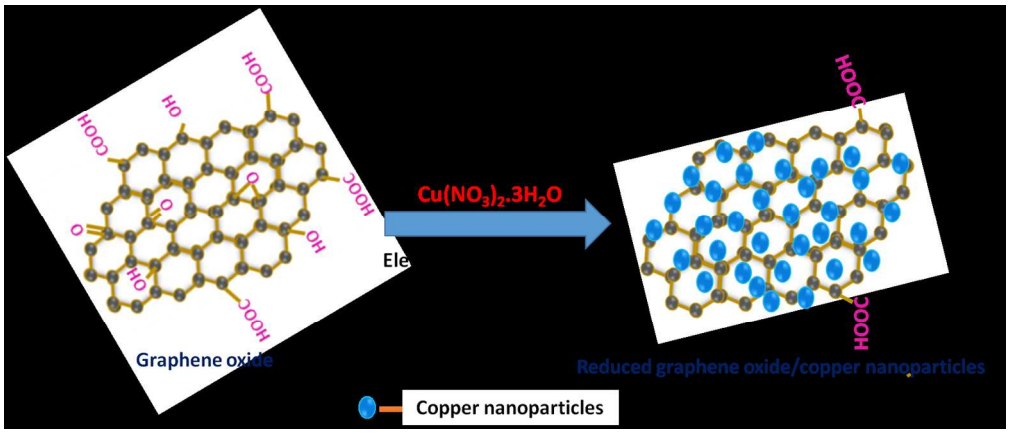

300x127mm (150 x 150 DPI)

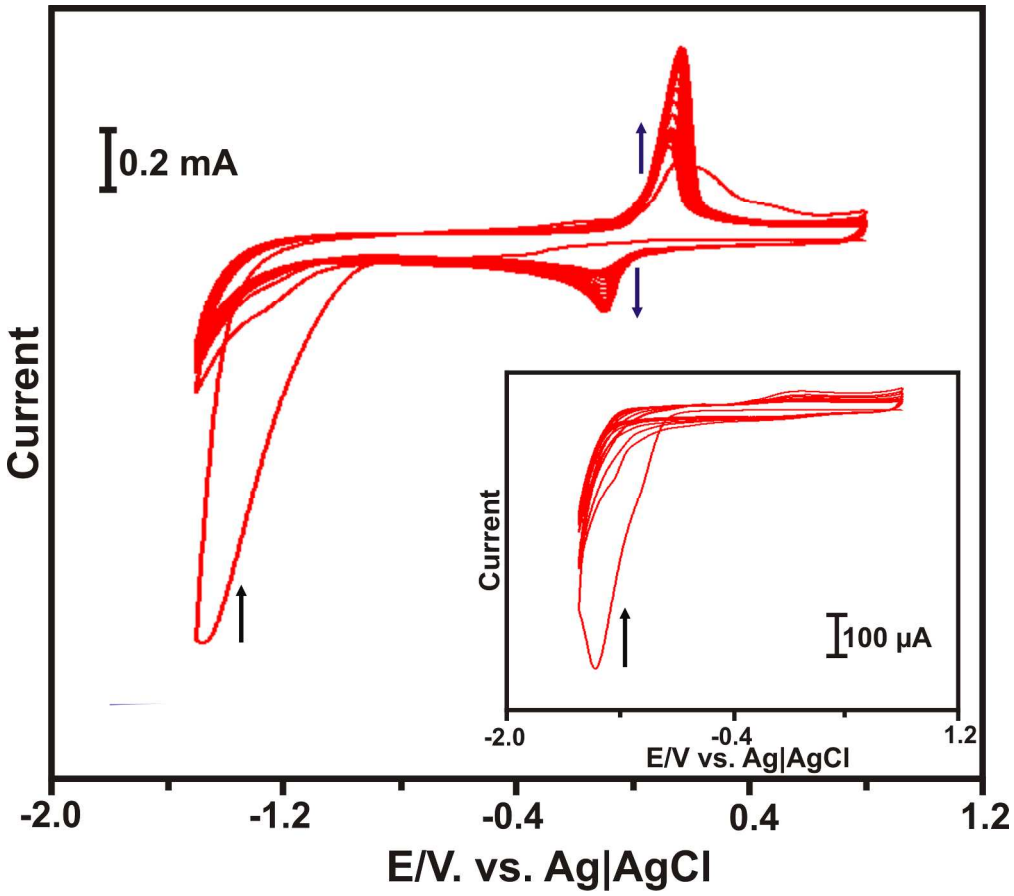

232x205mm (300 x 300 DPI)

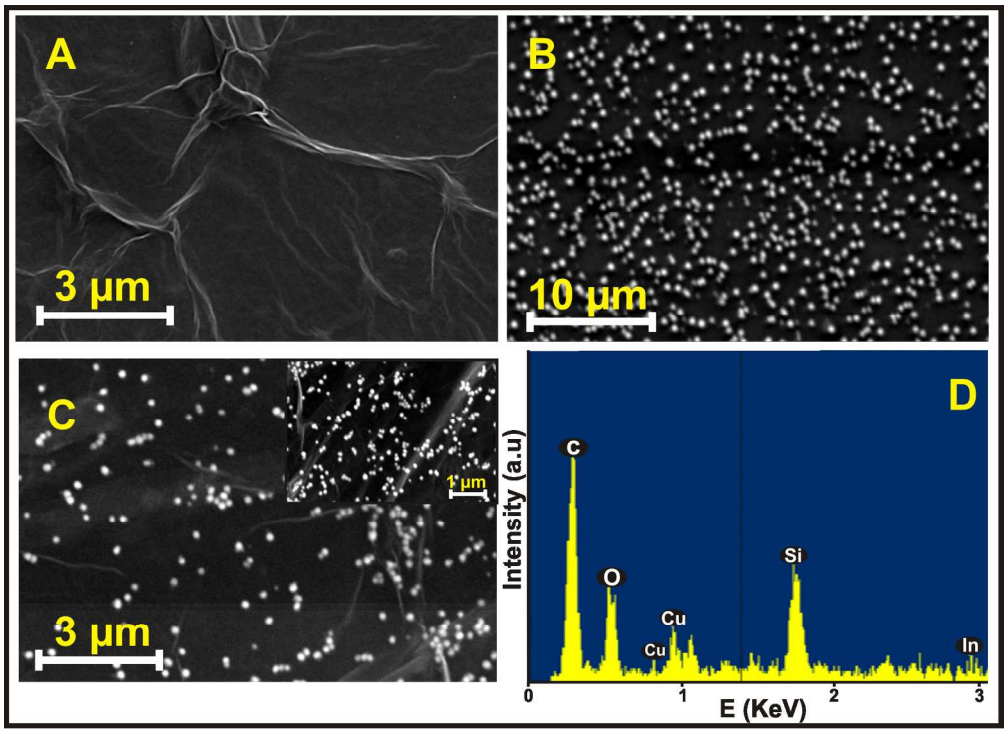

199x144mm (300 x 300 DPI)

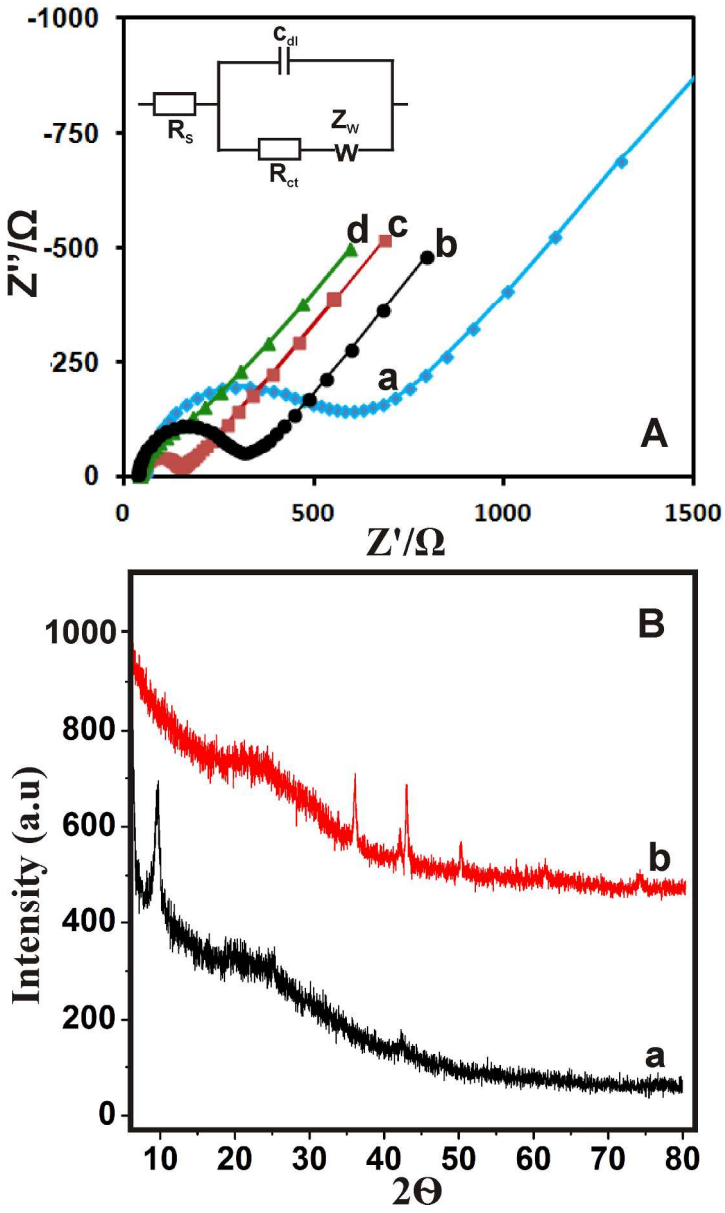

151x255mm (300 x 300 DPI)

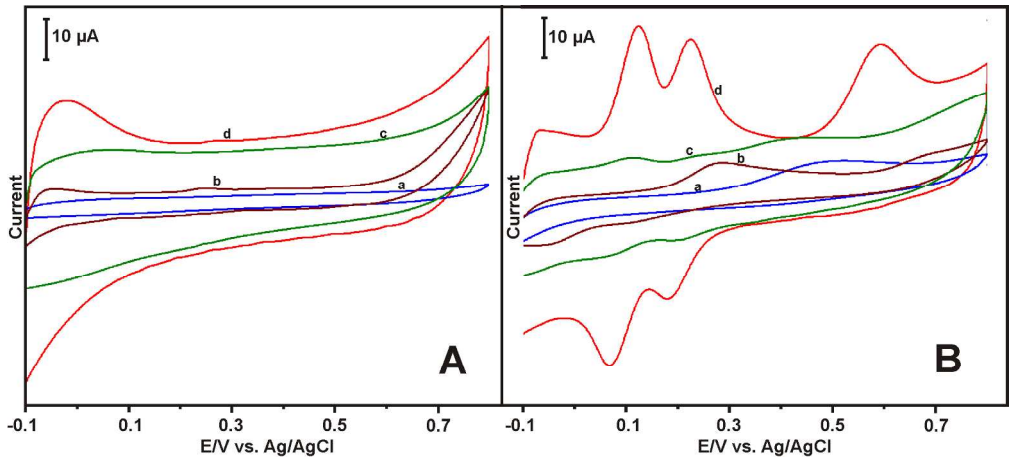

214x96mm (300 x 300 DPI)

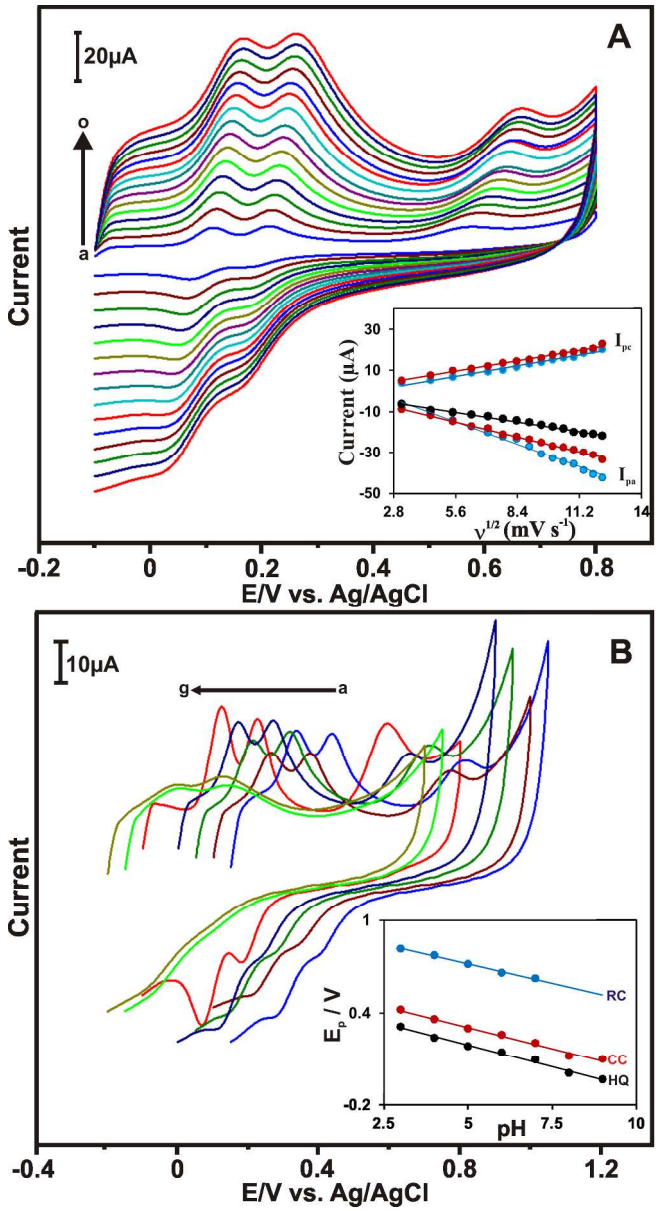

164x303mm (300 x 300 DPI)

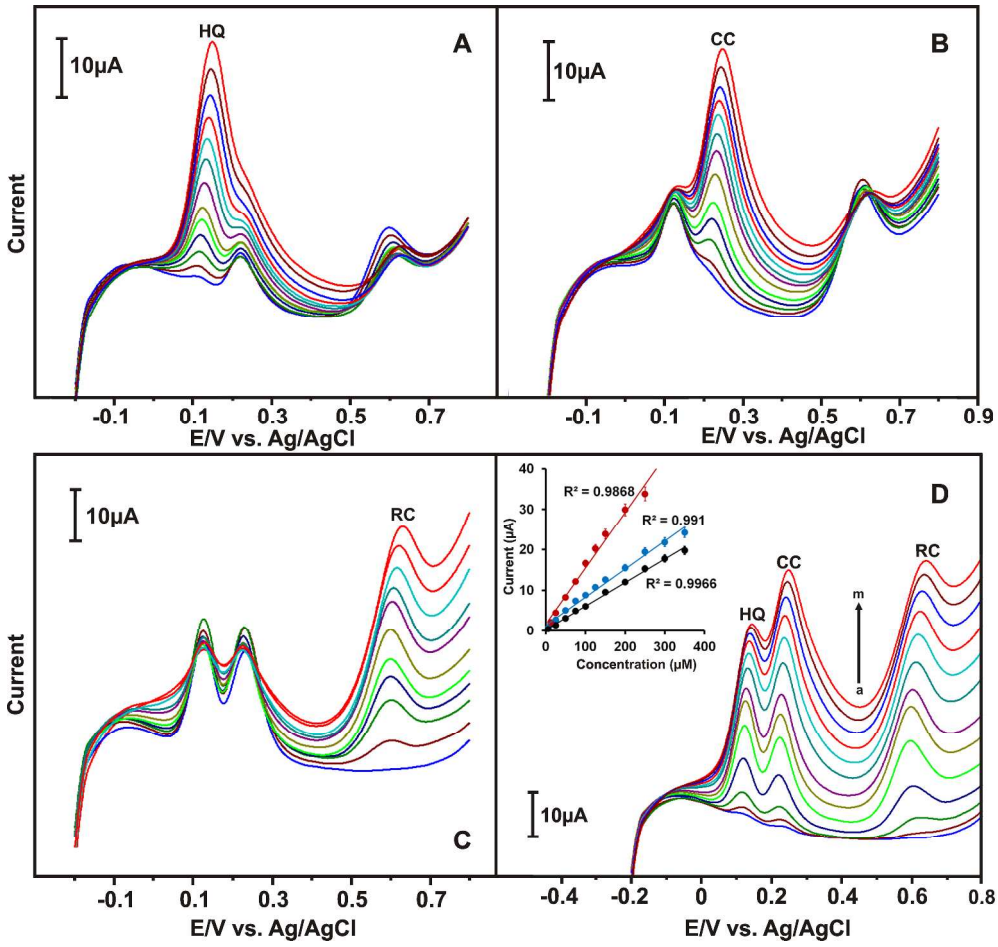

482x450mm (300 x 300 DPI)